High-Throughput Screening and Hit Validation of Extracellular-Related Kinase 5 (ERK5) Inhibitors

Stephanie M. Myers, Ruth H. Bawn, Louise C. Bisset, Timothy J. Blackburn, Betty Cottyn, Lauren Molyneux, Ai-Ching Wong, Celine Cano, William Clegg, Ross. W. Harrington, et al.

ACS Combinatorial Science

Research Article

pubs.acs.org/acscombsci

High-Throughput Screening and Hit Validation of Extracellular-Related Kinase 5 (ERK5) Inhibitors

Stephanie M. Myers,[†] Ruth H. Bawn,[†] Louise C. Bisset,[§] Timothy J. Blackburn,[†] Betty Cottyn,[†] Lauren Molyneux,[†] Ai-Ching Wong,[∥] Celine Cano,[†] William Clegg,[‡] Ross. W. Harrington,[‡] Hing Leung,[⊥] Laurent Rigoreau,[∥] Sandrine Vidot,[†] Bernard T. Golding,[†] Roger J. Griffin,[†] Tim Hammonds,[∥] David R. Newell,[§] and Ian R. Hardcastle*[,†]

[†]Newcastle Cancer Centre, Northern Institute for Cancer Research and School of Chemistry, Bedson Building, Newcastle University, Newcastle upon Tyne, NE1 7RU, U.K.

[‡]School of Chemistry, Newcastle University, Bedson Building, Newcastle upon Tyne, NE1 7RU, U.K.

[§]Newcastle Cancer Centre, Northern Institute for Cancer Research, Medical School, Framlington Place, Newcastle University, Paul O'Gorman Building, Newcastle upon Tyne, NE2 4HH, U.K.

[∥]Cancer Research Technology, Ltd., Discovery Laboratories, Wolfson Institute for Biomedical Research, The Cruciform Building, Gower Street, London, WC1E 6BT, U.K.

[⊥]The Beatson Institute for Cancer Research, Garscube Estate, Switchback Road, Bearsden, Glasgow G61 1BD, U.K.

Supporting Information

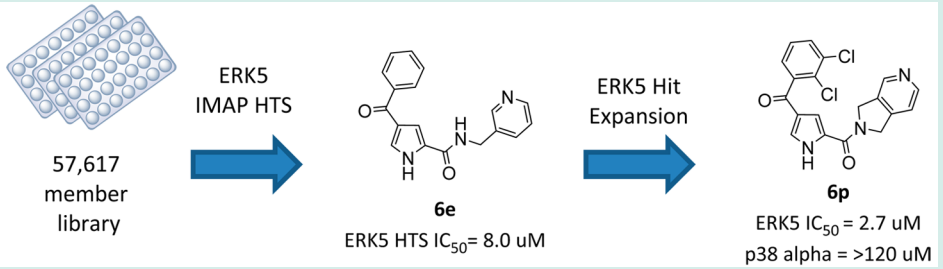

ABSTRACT: The extracellular-related kinase 5 (ERK5) is a promising target for cancer therapy. A high-throughput screen was developed for ERK5, based on the IMAP FP progressive binding system, and used to identify hits from a library of 57 617 compounds. Four distinct chemical series were evident within the screening hits. Resynthesis and reassay of the hits demonstrated that one series did not return active compounds, whereas three series returned active hits. Structure−activity studies demonstrated that the 4-benzoylpyrrole-2-carboxamide pharmacophore had excellent potential for further development. The minimum kinase binding pharmacophore was identified, and key examples demonstrated good selectivity for ERK5 over p38α kinase.

KEYWORDS: *extracellular-related kinase 5 (ERK5), cancer therapy, high-throughput screening, structure−activity studies, library, p38α kinase*

INTRODUCTION

The extracellular-related kinase 5 (ERK5), also known as big map kinase (BMK1), is a 816 amino acid protein kinase that forms part of a noncanonical MAP kinase pathway in cells.[1] Extracellular stimulation, in the form of growth factors, such as epidermal growth factor (EGF), nerve growth factor (NGF), vascular endothelium growth factor (VEGF), and fibroblast growth factor-2 (FGF-2), initiates a signaling cascade from the cell surface to nuclear transcription factors via ERK5.[2] Unlike the linear canonical Ras/Raf/MEK/ERK pathway, the ERK5 signaling cascade occurs independently of Raf.[3] ERK5 is activated specifically by MEK5, which is in turn activated by MEKK2/3.[1a,4]

ERK5 is structurally different from the other members of the ERK subfamilies. A unique loop-12 structure and extended C-terminal domain (~400 amino acids) gives ERK5 its characteristic structure.[2,4] The C-terminal extension harbors nuclear localization and export sequences, two proline-rich domains, a transcriptional activating domain, and MEF2 interacting region. The large C-terminal unique to ERK5 is autophosphorylated at multiple sites, resulting in an increase in transcriptional activity.[5]

Phosphorylation of ERK5 results in activation of a number of transcription factors including MEF2, c-Myc, c-Jun, c-Fos, Fra-1,

Received: October 14, 2015
Revised: June 13, 2016
Published: July 11, 2016

DOI: 10.1021/acscombsci.5b00155
ACS Comb. Sci. 2016, 18, 444−455

and NFκB.[6] ERK5 also phosphorylates and activates p90 RSK, also involved in signal transduction.[7] An increasing body of mechanistic data indicates that ERK5 plays a key role in tumor biology, that is, cell proliferation and survival, invasion and metastasis, and angiogenesis.[8]

Expression of ERK5 is significantly up-regulated in advanced prostate cancer and has been identified as an independent prognostic biomarker for aggressive disease.[9] ERK5 is overexpressed in 20% of breast cancer patients and its expression is an independent prognostic biomarker for reduced disease-free survival.[10] In hepatocellular carcinoma (HCC), ERK5 overexpression has been reported, associated with gene amplification at the 17p11 chromosome fragment, harboring the MAPK7 gene.[11] High levels of ERK5 were found to correlate with more aggressive and metastatic stages in fresh samples from human clear cell renal cell carcinoma.[12]

To date, three small-molecule inhibitors of the MEK5/ERK5 pathway have been described. The indolinone-based inhibitors, BIX02188 (**1a**) and BIX02189 (**1b**), are dual inhibitors of the MEK5/ERK5 cascade. Both compounds inhibit MEK5 with nanomolar potency, whereas modest activity was reported for ERK5.[13] Benzo[*e*]pyrimido-[5,4-*b*]diazepine-6(11*H*)-one (XMD8−92, **2**) is a potent ERK5 inhibitor which exhibits antiproliferative and antiangiogenic effects on HeLa cells in mouse xenograft models.[14] An X-ray crystal structure of **2** bound to ERK5 shows the inhibitor bound to the Met140 in the kinase hinge via a pair of hydrogen bonds from the aniline and pyrimidine nitrogens, and an additional water-bridged hydrogen bond from the diazepinone carbonyl to Asp200 and Glu102 in the DFG loop.[15] However, some of the in vivo activity of **2** has been attributed to off-target activities, for example, inhibition of doublecortin-like kinase 1 (DCLK-1) in pancreatic cancer.[16] Inhibition of ERK5 or siRNA knockdown has been shown to inhibit the growth of HCC cell lines, in vitro and in vivo.[17] ERK5 signaling has been shown to be essential for chemically induced carcinogenesis in skin by *erk5* gene deletion or ERK5 inhibition (with **2**).[18] The combination of doxorubicin and either *erk5* gene deletion or ERK5 inhibition (with **2**) was found to be additive in inflammation-driven tumor models. Thus, pharmacological inhibition of ERK5 may provide an opportunity for the treatment of inflammation-driven, invasive or metastatic cancers where ERK5 is deregulated. Given the strong link between ERK5 mediated signaling and malignancy, there remains a strong need to develop selective tool molecules to fully elucidate the effect of ERK5 inhibition in vivo. For this reason, we sought to discover novel ERK5 inhibitory chemotypes through high-throughput screening as chemical tools and for development as therapeutic agents.

In this Research Article, we describe the development of a high-throughput screening assay for ERK5 inhibition based on the IMAP FP format that was used to identify four discrete series of hit molecules. Validation of each series was attempted by resynthesis and retesting of selected members from each series. Preliminary structure activity studies were obtained resulting in the identification of one series for further optimization.

DEVELOPMENT AND EXECUTION OF ERK5 IMAP SCREEN

Assay Development. The discovery of kinase inhibitors using high-thoughput screening is well established.[19] In our case, expression of active ERK5 protein required coexpression of MEK5. The screen was developed using the IMAP format (Molecular Devices) that relies on the high specificity interaction

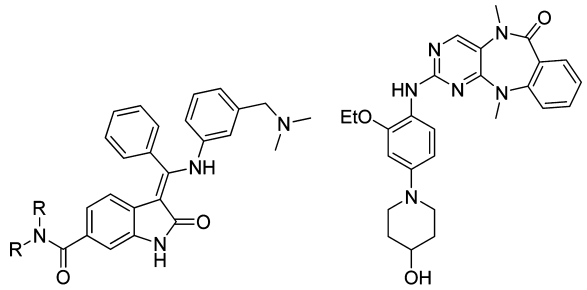

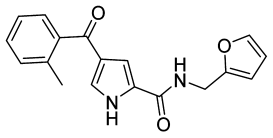

Table 1

number	sequence
166	5-FAM-AGRSPVD
168	5-FAM-EAGRSPVDS
170	5-FAM-HEAGRSPVDSL
172	5-FAM-RHEAGRSPVDSLS
174	5-FAM-TRHEAGRSPVDSLSS

Table 2

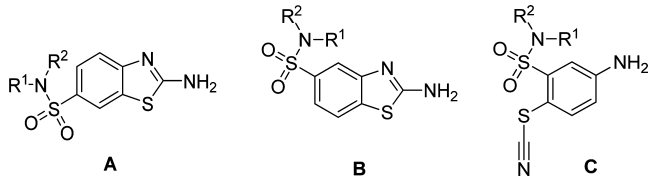

					ERK5 IC_{50} (μM)	
compound	structure	R^1		R^2	HTS	resynthesized[a]
3a	A	$-(CH_2)_4-$			0.057	51 ± 5.0
3b	A	Et		Me	0.087	85 ± 5.0
3c	A	Me		H	0.087	
3d	A	Et		H	0.11	
3e	A	$CH_2{=}CHCH_2-$		H	0.13	
3f	A	*s*-Bu		H	0.13	
3g	A	$-(CH_2)_5-$			0.46	
3h	A	*i*-Pr		H	0.60	
3i	A	*n*-Pr		H	0.89	>120[b]
3j	A	Et		Et	0.93	
3k	A	$-(CH_2)_2O(CH_2)_2-$			5.13	
9a	B	$-(CH_2)_4-$				29 ± 1.3
9b	B	Et		Me		21 ± 1.5
12a	C	$-(CH_2)_4-$				2.3 ± 1.5
12b	C	Et		Me		>120[b]

[a]Values are the mean of at least 3 determinations ± SD. [b]n = 2.

of phospho groups on a fluorescently tagged peptide with M^{3+} containing nanoparticles. The IMAP format was chosen as a robust and efficient method of determining kinase activity using a "mix-and-measure" format with a nonradioactive, fluorescence output.

Preliminary experiments to determine a suitable peptide substrate for the IMAP FP assay used a commercial source of the enzyme and were based on sequence of the natural substrate of ERK5, and were augmented with a substrate finder kit. Five

DOI: 10.1021/acscombsci.5b00155
ACS Comb. Sci. 2016, 18, 444−455

Table 3. ERK5 Inhibitory Activity of Nicotinonitrile Series 4a−k

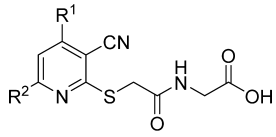

compd	R^1	R^2	ERK5 IC_{50} (μM) HTS	ERK5 IC_{50} (μM) Resynthesized[a]
4a	4-F-Ph	Ph	1.6	4.9 ± 0.3
4b	3-F-Ph	Ph		>120[b]
4c	2-F-Ph	Ph		34.3 ± 6.4
4d	Ph	Ph		>120[b]
4e	4-(CF_3)-Ph	Ph		>120[b]
4f	2,4-di-F-Ph	Ph		72.9 ± 26.1
4g	4-Py	Ph		65.1 ± 12.4
4h	4-MeOPh	Ph		>120[b]
4i	Ph	4-MeOPh		>120[b]
4j	Ph	CH_3		>120[b]
4k	CH_3	CH_3		>120[b]

[a]Values are the mean of at least 3 determinations ± SD. [b]n = 2.

peptide sequences were designed based around the reported site of phosphorylation of MEF2C by ERK5, with the expected serine phosphorylation site highlighted in red (Table 1).[1] The peptides were tested using the IMAP FP Progressive Binding System (Molecular Devices) in the absence and presence of ERK5 (Carna Biosciences).

The IMAP FP substrate finder kit for serine/threonine kinases plate 2 (molecular devices) covering CMGC, CK1, STE, and TKL portions of the kinome was used to identify potential peptide substrates phosphorylated by ERK5. The FAM-EGFR-derived peptide (LVEPLTPSGEAPNQK-5FAM-COOH) proved optimal.

Kinetic studies determined the ERK5 K_M^{app} to be 300 μM. Ideally, kinase screens are run with the ATP concentration equal to the K_M, however, in this case the IMAP format did not return acceptable results at a high ATP concentration (300 μM), presumably due to interference of ATP with the interaction of the phospho peptide with the metal nanoparticles. For this reason, the HTS assay was run at the maximum acceptable ATP concentration (100 μM) to allow "mix-and-measure" determinations.

High-Throughput Screening for ERK5 Inhibitors. To identify inhibitors of ERK5 the IMAP HTS assay was set up and a library of 57 617 small molecules was screened (final DMSO concentration of 4% and a total reaction volume of 40 μL). The library was composed of a 48 479 member diverse library and a 9136 member kinase focused library, both libraries were sourced from commercial vendors. Z' factors for each plate were calculated using eq 2, and were typically 0.6−0.8. Plates with Z' factors below 0.4 were rescreened (Supporting Information).

$$\frac{v}{[E]} = \frac{k_{cat}[S]}{(K_m + [S])} \quad (1)$$

$$Z' = 1 - \frac{3\sigma_{c+} + 3\sigma_{c-}}{|\mu_{c+} - \mu_{c-}|} \quad (2)$$

where σ and μ represent the standard deviation and mean of the positive (c+) and negative (c−) plate controls, respectively.

HTS Results. The HTS assay returned 245 active compounds (0.5% hit rate), that is, >50% inh at 30 μM, from the 57 617 member library. Active compounds (245) showing >50% inhibition in the screen were resupplied from stock or commercial vendors and retested at 30, 10, and 3.3 μM. 71 active compounds, giving >30% mean inhibition, were treated as confirmed hits (0.10% overall hit-rate) and assayed over a full IC_{50} range. IC_{50} determinations required a two stage process whereby the reaction occurred initially in the absence of the IMAP reagent, followed by subsequent addition of the IMAP reagent, to allow the K_M concentration of ATP to be used.

The hit compounds produced inhibition curves with IC_{50} values ranging from 0.6 to 76 μM (1 compound >120 μM). Confirmed hits were clustered according to common structures, revealing four promising chemical series. SAR around the hits was expanded by assaying related in-house compounds and close analogues from commercial suppliers. From these results, four compound series were selected for validation by resynthesis prior to progressing to hit-to-lead studies: 2-amino-*N*,*N*-alkylbenzo-[*d*]thiazole-6-sulfonamides (Table 2, **3a−c**), 4-substituted-2-(substitutedthio)-6-phenylnicotinonitriles (Table 3, **4a,b**), 4-amino-2-(arylamino)pyrimidine-5-carbonitriles (Table 5, **5a−c**), and 4-aroyl-*N*-alkyl-1*H*-pyrrole-2-carboxamides (Table 6, **6a−e**).

SYNTHESIS

Benzothiazole Series 3. Numerous methods have been described for the synthesis of benzothiazoles.[20] For the synthesis of compounds **3a** and **b** and analogues, we used the reported reaction of anilines with potassium thiocyanate-copper(II) sulfate (Scheme 1).[21] The required 4-aminophenylsulfonamides (**7a−c**) were prepared by reduction of the corresponding nitro compounds (**8a−c**). The nitro precursors were obtained by coupling the relevant amine with 4-nitrobenzenesulfonyl chloride. The 5-sulfonamide isomer **9a**, was prepared via the same method (Scheme 2). Thus, 3-nitrobenzenesulfonyl chloride was reacted with pyrrolidine or *N*-methylethylamine, and the resulting sulfonamides **10a** and **b** were reduced to the respective anilines **11a** and **b** (Scheme 2). Reactions of **11a** and **b** with with potassium thiocyanate-copper(II) sulfate gave in each

Scheme 1[a]

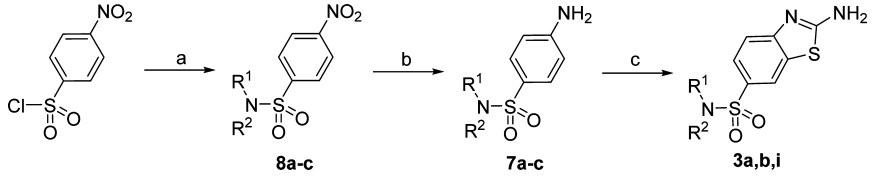

[a]Reagents and conditions: (a) pyrrolidine or *N*-methylethylamine or propylamine, Et_3N, DCM; (b) Pd/C, H_2, EtOAc; (c) KSCN, Cu(II)SO_4, MeOH.

DOI: 10.1021/acscombsci.5b00155
ACS Comb. Sci. 2016, 18, 444−455

Scheme 2[a]

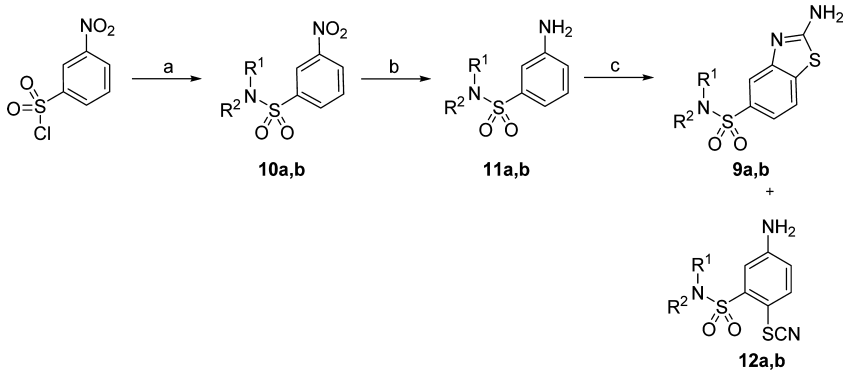

[a]Reagents and conditions: (a) pyrrolidine or *N*-methylethylamine, Et_3N, DCM; (b) Pd/C, H_2, EtOAc; (c) KSCN, $Cu(II)SO_4$, MeOH.

Scheme 3[a]

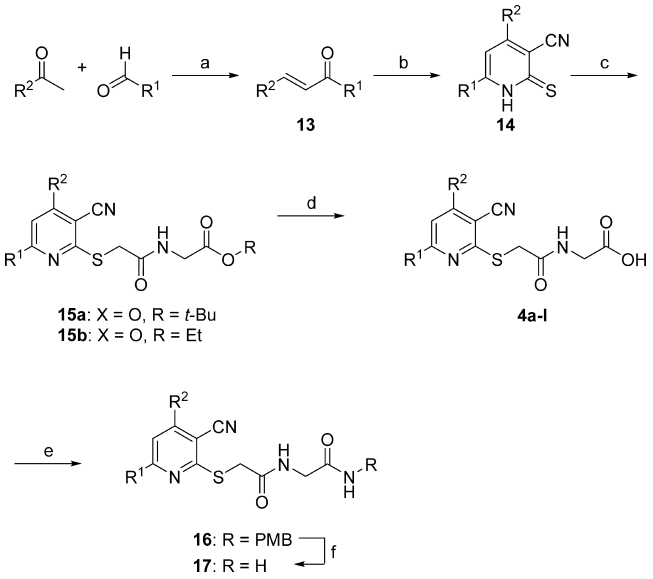

[a]Reagents and conditions: (a) KOH, EtOH, RT; (b) method A, S_8, morpholine, EtOH, 80 °C 30 min then malononitrile; or method B, 2-cyanothioacetamide, 1.6 M NaOMe in MeOH, 80 °C; (c) *tert*-butyl or ethyl 2-(2-bromoacetamido)acetate, K_2CO_3 or KOH, DMF, 100 °C; (d) TFA, RT; (e) *p*-methoxybenzylamine, HBTU, DIPEA, DMF, 60 °C; (f) TFA, 70 °C. NB: No base was required in step c after step b (method B), as an excess of NaOMe was used in step b

Scheme 5[a]

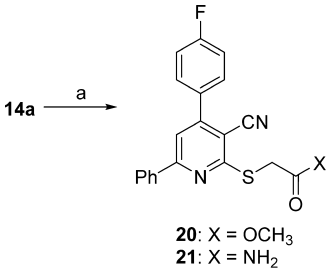

[a]Reagents and conditions: (a) methyl bromoacetate, KOH, DMF, reflux, or chloroacetamide, $NaOAc{\cdot}3H_2O$, ethanol, reflux.

Scheme 6[a]

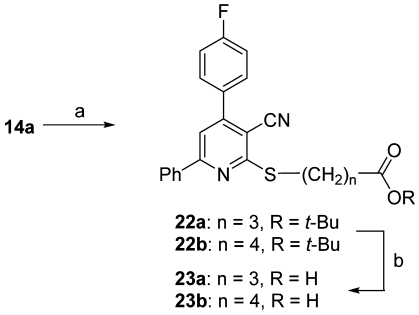

[a]Reagents and conditions: (a) RBr, K_2CO_3, THF, 100 °C; (b) TFA, RT.

case, besides the desired 5-substituted benzothiazole **9a** and **b**, a significant quantity of a thiocyanatobenzene (**12a** and **b**).

Nicotinonitrile Series 4. The first synthetic approach considered for the synthesis of 3-cyanopyridines was based on the route reported by Shestopalov et al.[22] For example, 4-fluorochalcone **13a**, prepared via Claisen−Schmidt condensation of acetophenone with 4-fluorobenzaldehyde, was treated

Scheme 4[a]

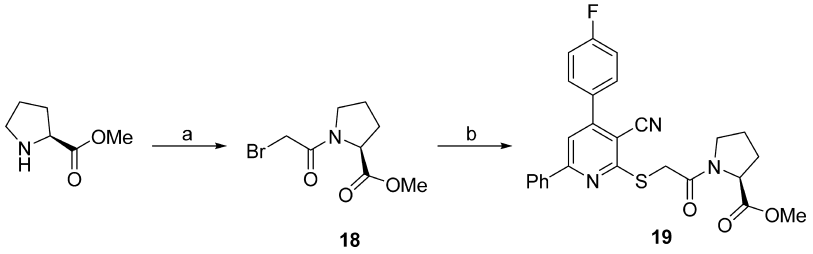

[a]Reagents and conditions: (a) bromoacetyl chloride, $CaCO_3$, $CHCl_3$, H_2O, 0 °C; (b) **14a**, KOH, DMF, reflux.

DOI: 10.1021/acscombsci.5b00155
ACS Comb. Sci. 2016, 18, 444−455

Scheme 7[a]

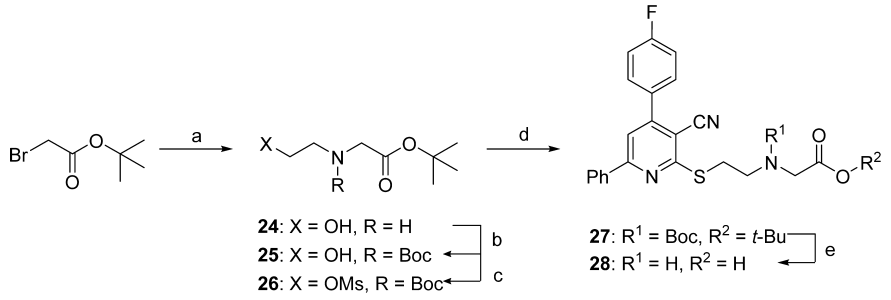

[a]Reagents and conditions: (a) ethanolamine, RT; (b) Boc_2O, Et_3N, DCM, 0 °C-RT; (c) MsCl, Et_3N, DCM, 0 °C-RT; (d) **14a**, DMF, 100 °C; (e) TFA, RT.

Scheme 8[a]

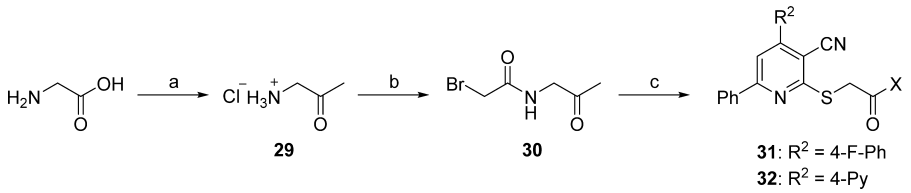

[a]Reagents and conditions: (a) (i) Ac_2O, pyridine, reflux; (ii) HCl, H_2O, reflux; (b) bromoacetyl chloride, $CaCO_3$, DCM, reflux; (c) **14a** or **14g**, K_2CO_3, DMF, 100 °C.

Scheme 9[a]

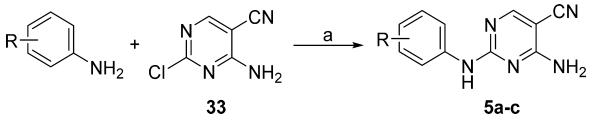

[a]Reagents and conditions: (a) DMF, 100 °C.

Scheme 10[a]

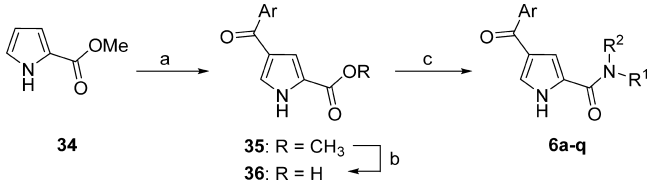

[a]Reagents and Conditions: (a) ArCOCl, $AlCl_3$, DCM, 0 °C-RT; (b) LiOH, THF, H_2O, 60 °C; (c) (i) CDI, THF, 70 °C; (ii) R^1R^2NH, 50 °C–RT.

with elemental sulfur and morpholine in ethanol at reflux, followed by malononitrile, to give pyridinethione **14a** in moderate yield (Method A, Scheme 3). Isolation of the intermediate pyridinethiones **14** required extensive purification, attributed to the propensity of this intermediate to tautomerise, and its readiness to oxidize under atmospheric conditions.

Consideration of the likely mechanism of the one-pot sequence of the cyclization reaction prompted the replacement of the sulfur and malononitrile with 2-cyanothioacetamide for the Michael addition in an alternative route (Method B, Scheme 3). Reactions were performed under nitrogen to avoid oxidative side-reactions. The crude intermediate **14** was used directly in the alkylation step, to avoid a lengthy purification, giving cyanopyridines **15a–k**. Method B allowed isolation of **15a** in an improved 54% yield over 2 steps. Deprotection with TFA gave acids **4a–k** in near quantitative yield (99%). The carboxamide **17** was prepared from **4a** by a HBTU-mediated coupling with *p*-methoxybenzylamine giving amide **16**, which was deprotected with TFA.

Further variations to the thioether group were introduced via alkylation of **14a** (Schemes 4–7). The acetamide derivatives **31** and **32** were prepared by the alkylation of **14a** and **14g**, respectively, with bromoacetamide **30**, which was obtained by reaction of aminoacetone hydrochloride **29** with bromoacetyl chloride (Scheme 8).[23]

Scheme 11[a]

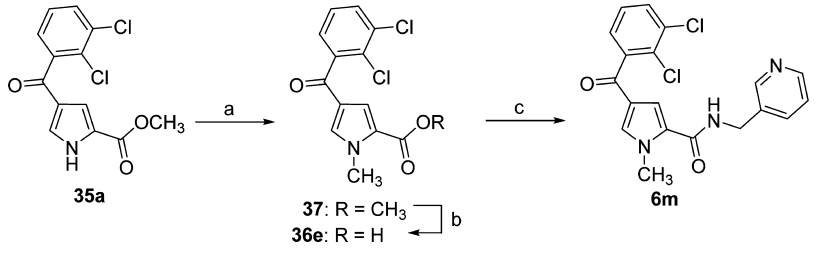

[a]Reagents and conditions: (a) NaH, DMF, MeI; (b) LiOH, THF, H_2O, 60 °C; (c) (i) CDI, THF, 70 °C; (ii) 3-pyridylmethylamine, 50 °C–RT.

DOI: 10.1021/acscombsci.5b00155
ACS Comb. Sci. 2016, 18, 444–455

Scheme 12[a]

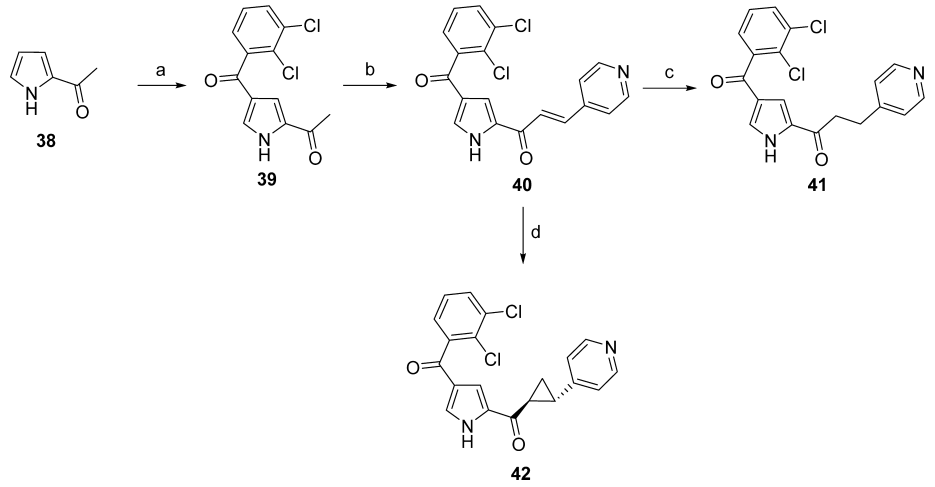

[a]Reagents and Conditions: (a) $AlCl_3$, 2,3-dichlorobenzoyl chloride, DCM, 0 °C-RT, 18 h; (b) isonicotinaldehyde, KOH, EtOH, H_2O, 0 °C−RT, 18 h; (c) indium powder, NH_4Cl, EtOH, H_2O, reflux, 8 h; (d) $(CH_3)_2SO^+I^-$, KO^{t}Bu, DMSO, RT, 24 h.

Scheme 13[a]

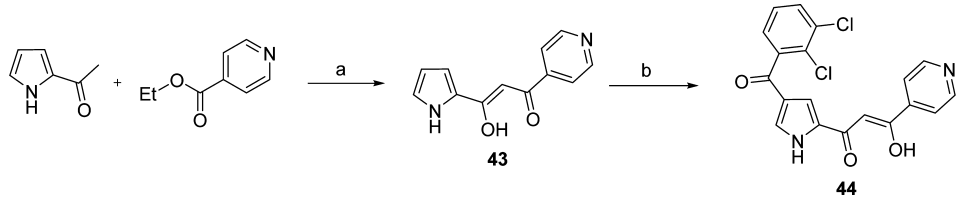

[a]Reagents and conditions: (a) KO^{t}Bu, THF, RT, 6 h; (b) $AlCl_3$, 2,3-dichlorobenzoyl chloride, DCM, 0 °C-RT, 18 h.

Cyanopyrimidine Series 5. A small series of 4-amino-2-anilinopyrimidine-5-carbonitriles (**5a**−**c**) were prepared by the reaction of the appropriate aniline with chloropyrimidine (**33**) at 100 °C in DMF (Scheme 9).[24]

4-Benzoylpyrrole-2-carboxamide Series 6. A selection of 4-benzoylpyrrole-2-carboxamides were prepared by Friedel−Crafts acylation of methyl 1*H*-pyrrole-2-carboxylate (**34**) with a substituted benzoyl chloride giving pyrrole (**35**). Hydrolysis of the methyl ester with lithium hydroxide gave carboxylic acid **36** that was coupled with the appropriate amine using CDI to give the desired carboxamides (**6a**−**r**) (Scheme 10). The *N*-methyl derivative **6m** was prepared by methylation of ester **35a**, followed by hydrolysis and coupling with 3-pyridylmethylamine (Scheme 11).

2-Substituted-4-benzoylpyrrole Derivatives. The alkene derivative **40** was prepared by aldol condensation of ketone **39** and isonicotinaldehyde (Scheme 12). Selective reduction was achieved by refluxing alkene **40** in aqueous ethanol with indium metal and ammonium chloride giving alkane **41** in moderate yield.[25] The cyclopropyl analogue **42** was prepared by a Corey Chaykovsky reaction.[26] Thus, alkene **40** was reacted with trimethylsulfoxonium iodide and potassium *tert*-butoxide giving **42** in 12% yield.[27] Diketone **44** was prepared via a Claisen condensation between 1-(1*H*-pyrrol-2-yl)ethanone and methyl isonicotinate diketone **43** (Scheme 13). Friedel−Crafts acylation with 2,3-dichlorobenzoyl chloride gave **44**.

DISCUSSION

Selected examples of the HTS hits in the benzothiazole series (**3a**, **3b**, **3i**) were synthesized and reassayed. The ERK5 inhibitory activity for the resynthesized benzothiazoles were 1000-fold lower than for the library material (Table 2). Comparison of the ^{1}H NMR and LCMS spectra of the resynthesized and screened samples of **3a** suggested that the library material was the 5-sulfonamide **9a**, so authentic samples of isomers **9a** and **9b** were prepared. In order to eliminate the possibility of mis-identification of the compounds by spectroscopic methods, the identity of isothiocyanate **12a** and benzothiazoles **3a** and **3i** were elucidated by small-molecule X-ray crystallography (Figures 1−3).

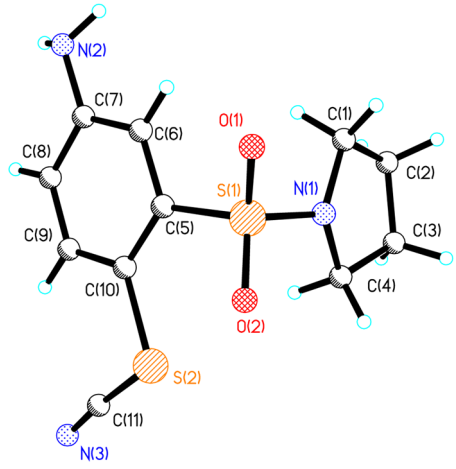

Figure 1. Crystal structure of 3-(pyrrolidin-1-ylsulfonyl)-4-thiocyanatobenzenamine **12a**.

DOI: 10.1021/acscombsci.5b00155
ACS Comb. Sci. 2016, 18, 444−455

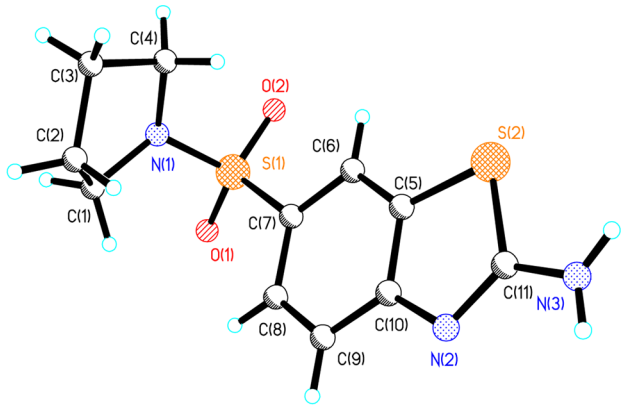

Figure 2. Crystal structure of 6-(pyrrolidine-1-sulfonyl)-benzothiazol-2-ylamine **3a**.

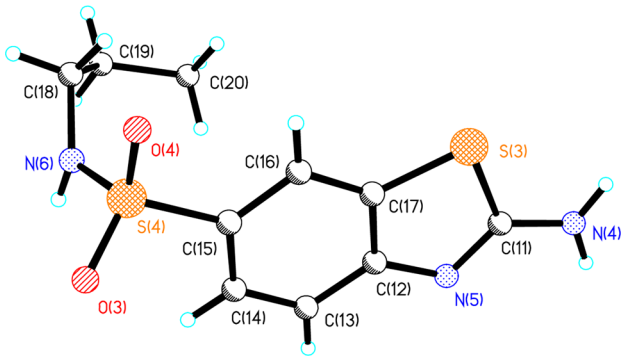

Figure 3. Crystal structure of 2-amino-*N*-propylbenzo[*d*]thiazole-6-sulfonamide **3i**.

The assay results for these isomers also failed to replicate the initial IC_{50} values from the screening samples. Interestingly, the isothiocyanate side-product **12a** showed 10-fold greater potency than the benzothiazole, although this result was not replicated for the analogue **12b**. Time-dependent enzyme inactivation by isothiocyanates, via their reaction with lysine residues, has been reported.[28] Further investigations into the mechanism of action of **12a** were not conducted. Some aminothiazoles have recently been identified as frequent hitters from a fragment screening set and dubbed promiscuous 2-aminothiazoles (PrATs).[29] The reason for the discrepancy between the activity of the HTS sample and the resynthesized material is not clear. Numerous mechanisms for false positives in HTS are possible, including the presence of trace impurities or protein aggregation, and further effort was not expended eliminating these possibilities.[30]

Three HTS hits in the nicotinonitrile series (**4a**, **19**, and **31**) were synthesized and reassayed (Tables 3 and 4). The results for the glycine derivative **4a** and proline methyl ester derivative **19** were in good agreement with the HTS IC_{50} values. In contrast, the propan-2-one derivative **31** was 50-fold less active than the HTS result. On this basis, a limited series of compounds was prepared to establish preliminary SARs and to determine the minimum inhibitory pharmacophore. The SARs for the 4- and 6-substitutents were delineated keeping the 2-thio substituent as the glycine amide (Table 3). The 4,6-diphenyl, 4-phenyl-6-methyl, and 4,6-dimethyl compounds (**4d**, **4j**, and **4k**, respectively) were each devoid of activity. The 4-(2-fluorophenyl) derivative **4c** was 7-fold less active than the 4-(4-fluorophenyl) derivative **4a**, whereas the 4-(3-fluorophenyl) derivative **4b** lacked measurable potency. The combination of 2-fluoro and 4-fluoro substituents (**4f**) was not additive and resulted in a 15-fold loss of potency compared with **4a**. The 4-(4-pyridyl) derivative **4g** exhibited a 13-fold loss in potency compared to **4a**, despite the similar electronic properties of the rings. Substitution of the 4-phenyl group with 4-trifluoromethyl **4e**, or 4-methoxy **4h** resulted in loss of activity.

The SARs for the thioether side-chain were investigated (Table 4). The pyridine thiol **14a** lacking the amide side-chain showed a 20-fold loss in potency compared to **4a**. The glycine ethyl ester **15l** showed similar activity to the proline methyl ester derivative **19**, and was 4-fold less potent than the corresponding glycine derivative **4a**. In contrast, the glycine amide **17** lacked

Table 4. ERK5 Inhibitory Activity of Nicotinonitrile Series 14a, 15l, 17, 19−21, 23, 28, and 31−32

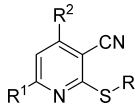

Compound	R	R^1	R^2	ERK5 IC_{50} (μM)	
				HTS	Resynthesized[a]
14a	H	Ph	4-F-Ph	-	111 ± 6.5
15l	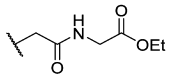	Ph	4-F-Ph	-	20.9 ± 1.6[c]
17	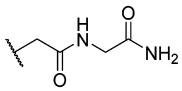	Ph	4-F-Ph	-	>120
19	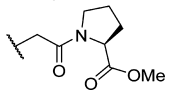	Ph	4-F-Ph	31	29.4 ± 3.7[c]
20	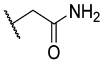	Ph	4-F-Ph	-	117 ± 18
21	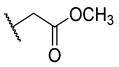	Ph	4-F-Ph	-	>120
23a	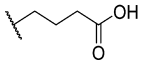	Ph	4-F-Ph	-	>120[d]
23b	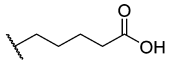	Ph	4-F-Ph	-	>120[d]
28	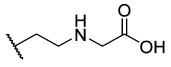	Ph	4-F-Ph	-	>120
31	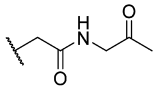	Ph	4-F-Ph	0.4	20.5 ± 1.3
32	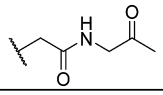	Ph	4-Py	-	104.9 ± 6.5

[a]Values are the mean of at least 3 determinations ± SD. [b]n = 1. [c]n = 2. [d]precipitation observed at 1.2 mM in 40% DMSO.

Table 5. ERK5 Inhibitory Activity of Pyrimidine Series 5a−c

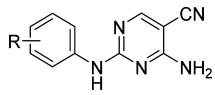

compound	R	ERK5 IC_{50} (μM)	
		HTS	resynthesized[a]
5a	2-CH_3	26	88 ± 3
5b	3-OCH_3	11	23 ± 7
5c	4-F	6.5	12 ± 3

[a]Values are the mean of at least 3 determinations ± SD.

DOI: 10.1021/acscombsci.5b00155
ACS Comb. Sci. 2016, 18, 444−455

Table 6. ERK5 Inhibitory Activity of Pyrrole Carboxamides (6a−e)

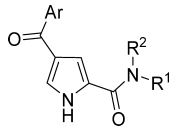

Compound	Ar	R^1	R^2	ERK5 IC_{50} (μM)	
				HTS	Resynthesized[a]
6a	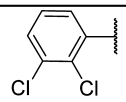	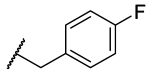	H	0.66	3.7
6b	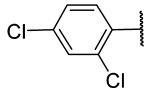	CH_3	CH_3	1.89	>120[b]
6c	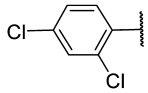	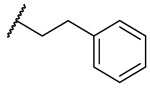	H	3.50	>120[b]
6d	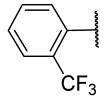	CH_3	H	4.32	9.6 ± 3.9
6e	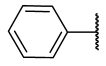	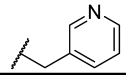	H	8.0	26.0 ± 1.2

[a]Values are the mean of at least 3 determinations ± SD. [b]n = 2.

measurable activity. The shorter, unsubstituted amide **20** showed weak activity, whereas the corresponding ester **21** was inactive. Two thioalkyl carboxylic acids **23a** and **23b** were inactive, as was the corresponding amine **28**, demonstrating the requirement for the amide group in the side chain for potency. Comparison of the 4-fluorophenyl propan-2-one derivative **31** with the 4-pyridyl derivative **32** showed a 5-fold loss in potency consistent with the results in the glycine amide series (**4a** and **4g**).

Overall, each of the changes made to the hit compounds in the nicotinonitrile series (**4a**, **19**, and **31**) resulted in loss of potency. Modifications to the aromatic and side-chain substituents revealed a highly constrained pharmacophore and limited SAR. As a result, no further optimization of this series was attempted. Interestingly, 3-cyano-4,6-diphenyl-pyridines have been identified recently as inhibitors of the PA−PB1 protein−protein interaction for influenza.[31]

The cyanopyrimidines **5a−c** showed reasonable activity against ERK5, with IC_{50} values in the 12−88 μM range (Table 5), and generally consistent with the HTS values. The activity against ERK5 in this series was promising, but the series had also been selected for development against another target internally. For this reason, no further analogues were prepared. Kinase inhibitors incorporating a 5-cyanopyrimidine core have been reported, for example, Wee1 inhibitors[32] and CDK2 inhibitors.[33]

Five 4-benzoylpyrrole-2-carboxamides (**6a−e**) gave good potency in the HTS. Upon resynthesis and retesting, the 2,3-dichlorobenzoyl-*N*-(4-fluorobenzyl) substitued analogue **6a** maintained significant activity (IC_{50} = 3.7 μM) despite a 5-fold loss in potency compared to the HTS result (Table 6). Similarly, the 2-trifluoromethylbenzoyl-*N*-methyl substituted analogue **6d** gave a 2-fold drop in activity (IC_{50} = 9.6 μM) compared to the HTS result, and the benzoyl-*N*-methyl-3-pyridyl derivative **6e** gave a 3-fold drop in activity (IC_{50} = 26 μM). In contrast, the resynthesized 2,4-dichlorobenzoyl analogues **6b** and **6c** bearing either the *N*,*N*-dimethylamide or *N*-phenethylamide substituents, respectively, showed no activity.

Encouraged by these results, a small series of aroylpyrroles was prepared. Compounds were designed to establish the minimum kinase binding pharmacophore, and to explore possibilities to gain potency and selectivity by variation of the amide substituent. The benzoyl substituent was fixed as the most potent 2,3-dichlorophenyl for all these examples.

Series (**6f−n**) was prepared to explore simple variations to the amide moiety (Table 7). Monomethyl amide **6f** was equipotent with the parent 4-fluorobenzyl amide **6a**, whereas the dimethyl amide **6g** was 7-fold less potent. Introduction of the 3-pyridylmethyl amide from **6e** or the 4-pyridylmethyl amide **6h**, retained potency, whereas the benzyl derivative **6k** and 2-pyridyl derivative **6j** were less potent, and phenylethyl amide **6l** was inactive. Similar to **6g**, *N*-methyl-(3-pyridylmethyl) amide derivative **6n** was 7-fold less potent than primary amide **6i**. Importantly, methylation of the pyrrole NH (**6m**) completely abolished ERK5 activity, indicating an essential interaction with the kinase at this position. In contrast, the relatively small drop in activity for the secondary amides **6g** and **6n** suggested the amide NH was not forming a critical interaction, and that the drop in potency could be related to the conformational preference of the amide group. With this in mind, a limited number of conformationally restricted, 5- and 6-membered cyclic secondary amides were investigated (Table 8). The 3,4-dihydro-2,6-naphthyridinyl and isoindolinyl derivatives (**6o** and **6q**) were inactive. In contrast, 3,4-dihydroisoquinolinyl **6p** was 5-fold less potent than **6h**, a comparable to the loss in potency seen for the *N*-methyl analogues, whereas the pyrrolidinopyridinyl **6r** was equipotent with **6h**. Selected examples in this series were assayed in an orthogonal LANCE assay format (see Supporting Information), based on time-resolved fluorescence resonance energy transfer (FRET), to eliminate the possibility of false positives. In all cases, the LANCE results were comparable with those obtained using the IMAP assay.

To establish the minimum kinase binding pharmacophore, systematic isosteric replacements to the amide group were made.

DOI: 10.1021/acscombsci.5b00155
ACS Comb. Sci. 2016, 18, 444−455

Table 7. ERK5 SAR for Pyrrole Carboxamides (6f−n)

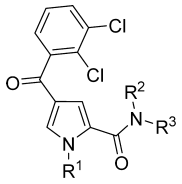

Compound	R^1	R^2	R^3	ERK5 IC_{50} (μM) IMAP[a]	ERK5 IC_{50} (μM) LANCE[a]
6f	H	H	CH_3	3.3 ± 1.0[b]	3.6 ± 1.0
6g	H	CH_3	CH_3	24 ± 27[c]	44 ± 24
6h	H	H	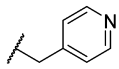	2.0 ± 2.0[d]	-
6i	H	H	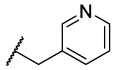	3.8 ± 3.7[c]	1.1 ± 0.4[c]
6j	H	H	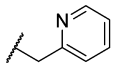	7.2 ± 0.02	3.9 ± 0.8
6k	H	H	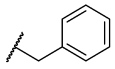	21[e]	-
6l	H	H	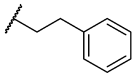	>120	-
6m	CH_3	H	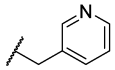	>120	-
6n	H	CH_3	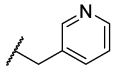	25 ± 1.3	13 ± 1.9

[a]Determinations ± standard deviation (mean of $n = 2$ unless otherwise stated). [b]IC_{50} mean of $n = 4$; [c]IC_{50} mean of $n = 6$; [d]IC_{50} mean of $n = 10$; [e]IC_{50} $n = 1$.

The acetyl derivative **39** and the 1,3-diketone **44** were inactive (Table 9). In contrast, the unsaturated ketone **40** and the cyclopropyl ketone **42** retained similar activity to the parent **6a**, whereas the saturated ketone **41** was 10-fold less active. These results confirm that the amide NH is not required for activity, and that conformational rigidity at this position is favorable. The loss of activity for diketone **44** was explained by the preferred enol tautomer lacking an essential H-bond to the kinase via the ketone adjacent to the pyrrole.

The most potent pyrrole inhibitor **6h** was submitted for a kinase selectivity screen and gave a promising selectivity profile. Of the 20 kinases, screened only one kinase (SAPK2a or p38α MAP kinase) was inhibited at >50% inhibition (10 μM). Subsequent to our identification of pyrrole-2-carboxamides as ERK5 inhibitors, similar compounds, e.g. **45**, have been independently identified as p38α MAP kinase inhibitors with micromolar activity.[34] The X-ray structure of **45** shows it bound to the hinge of the kinase via hydrogen bonds from the pyrrole NH and the carboxamide carbonyl, with the aryl portion occupying the lipophilic region close to the gatekeeper, and the furan binding in the outer lipophilic region. ERK5 shares 48% sequence homology with p38α MAP kinase, and 58% homology in the kinase domain. In addition, the gatekeeper residues of the kinases are similar, with leucine in ERK5 and threonine in p38α MAP kinase. The ERK5 SAR for our series is consistent with a similar binding mode to ERK5 as seen in the p38 X-ray structure, in particular the donor/acceptor doublet of H-bonds from the pyrrole NH and amide carbonyl to the kinase.

At this point, given the similarity between the published p38α MAP kinase inhibitors and our hit series, we needed to establish selectivity vs p38α MAP kinase to provide useful ERK5 tool compounds or therapeutic agents.[34,35] Thus, selected compounds were counterscreened against p38α MAP kinase using a LANCE assay. As anticipated, the 2-pyridyl derivatives **6j** and 3,4-dihydroisoquinolinyl derivative **6p** were equipotent for both p38α MAP kinase and ERK5. Importantly, the pyrrolidinopyridinyl derivative **6r** was inactive in the p38α assay. The ability to eliminate p38α MAP kinase activity while maintaining ERK5 activity by variation of the amide side chain was not readily predicted from the published p38α X-ray structure and points to differing structural requirements around the amide side-chain that may be exploited in further development of the series.

CONCLUSIONS

The IMAP FP high-throughput screen for ERK5 returned four distinct chemical series as hits. Synthesis of the hits and selected close analogues demonstrated that the HTS activity of the benzothiazoles **3** was not reproducable, activity for the cyanopyridine hits (**4a**, **19**) was reproducable, but the limited scope to develop the SAR ruled this series out, and two series with confirmed active hits. The lack of activity of these hits was disappointing but not atypical in screening campaigns. The cyanopyrimidine hits **5a−c** were not pursued for reasons of competition. The remaining series, the pyrrole carboxamides **6a−e**, demonstrated consistent ERK5 activity, with SARs consistent with a kinase hinge binder. Selectivity against the close homologue p38α MAP kinase was achieved without loss of ERK5 activity through minor structural modification, and a representative example **6h** showed an acceptable kinase selectivity profile in a panel. At this stage the pyrrole carboxamides demonstrated tractable synthesis, intelligible preliminary SARs, and promising selectivity. The relatively modest kinase inhibitory activity achieved at this stage did not give any concern as the pharmacophore established presented opportunities to optimize potency at both the benzoyl and amide portions, indepenently. Having demonstrated the necessary requirements to progress to the hit-to-lead optimization stage, further SAR studies were undertaken, with an initial focus on improving potency, which will be reported separately.[36]

EXPERIMENTAL PROCEDURES

IMAP Substrate Mapping. Nonphosphorylated and phosphorylated versions of each ERK5 sequence (Table 1) were obtained from the CRUK Peptide Synthesis Research Services group. The substrate finder kit was used according to the manufacturer's instructions. Reaction buffer (10 μL) containing ATP (100 μM) was added to wells of the plate to reconstitute 5-FAM labeled substrates. Reaction buffer (10 μL) with or without ERK5 (6.4 ng/μL) was added to appropriate wells of the plate, to generate background controls and positive controls. The reaction was incubated for 1 h at ambient temperature after which IMAP Binding Solution (60 μL) was added. After a further 1 h of incubation the fluorescence polarization was measured. The results were analyzed using the IMAP Substrate Mapper provided with the kit.

Kinetic Characterization of ERK5. Reactions were carried out with varying concentrations of ATP at constant substrate and

DOI: 10.1021/acscombsci.5b00155
ACS Comb. Sci. 2016, 18, 444−455

Table 8. SAR for Cyclic Pyrrole Carboxamides (6j, 6o−r) against ERK5 and p38α

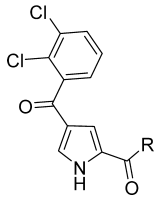

Compound ID	R	ERK5 IC50 (μM)[a]		p38α LANCE IC_{50} (μM)[a]
		IMAP	LANCE	
6j	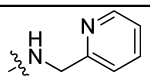	7.2 ± 0.03		4.3 ± 1.2[b]
6o	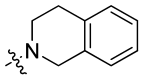	>120	-	
6p	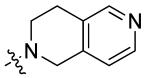	11 ± 2.3[b]	25 ± 1.8	28 ± 20
6q	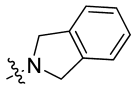	>120	-	
6r	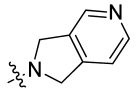	2.7 ± 0.4	-	> 120

[a]Determinations ± standard deviation (mean of n = 2 unless otherwise stated). [b]IC_{50} mean of n = 4.

Table 9. ERK5 SAR for Pyrroles (39−42, 44)

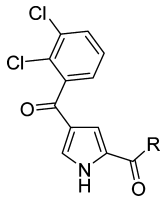

Compound ID	R	ERK5 IC_{50} (μM)[a]	
		IMAP	LANCE
39	CH_3	>120	-
40	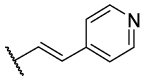	3.1 ± 0.1[b]	-
41	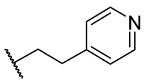	23 ± 4.4	24 ± 2.2
42	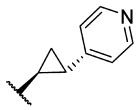	6.8 ± 2.0	16 ± 5.7[c]
44	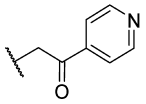	>120	-

[a]Determinations ± standard deviation (mean of n = 2 unless otherwise stated). [b]Mean of n = 4. [c]Mean of n = 6.

enzyme concentrations. Because of limitations of the IMAP FP assay with respect to ATP concentrations, we utilized a transfer method to increase the maximum concentration of ATP that can be used. Reactions were conducted as normal in 10 μL reaction volume. After either 1, 2, 3, or 4 h incubation period at 37 °C, 4 μL of the reaction was transferred to 196 μL of reaction buffer followed by a subsequent transfer of 10 μL of this solution to 30 μL of IMAP Binding Solution. Rates of reaction at 1 h reaction time at the range of substrate concentrations were determined, and kinetic parameters were determined by nonlinear regression fitting of the data to the Michaelis−Menten eq (eq 1) ; curve fitting was performed using GraphPad Prism software.[37]

ERK5 High-Throughput Screen. Compounds were assayed in a 10 μL reaction mixture per well containing: 1 in 700 dilution of ERK5 stock from CRT, 100 nM peptide R7129 and 100 μM of ATP. The reactions were performed with 10 mM Tris-HCl (pH 7.2), 10 mM $MgCl_2$, 0.05% NaN_3, and 0.01% Tween-20. Reactions were incubated for 3 h at 37 °C, followed by addition of 30 μL of IMAP binding solution (1 in 600 dilution of IMAP binding reagent in 60% Binding Buffer A and 40% Binding Buffer B) and a further incubation for 2 h at ambient temperature. Plates were read on an Analyst HT microplate reader and the data analyzed using ActivityBase.

ERK5 IC_{50} Determination (IMAP). The enzyme reaction was run as described for the HTS but using 300 μM ATP, 250 nM peptide and a reduced incubation time of 2 h at 37 °C. One μL of this reaction was then transferred to a new assay plate and 9 μL of reaction buffer was added followed by 30 μL of IMAP binding solution.

X-ray Crystallography. Data were collected on an Oxford Diffraction Gemini A Ultra diffractometer for **3i**, using MoKα radiation (λ = 0.71073 Å) at 150 K, and on a Bruker Apex2 diffractometer for **3a** and **12a**, using synchrotron radiation (λ = 0.6946 Å; SRS station 9.8, Daresbury Laboratory) at 120 K

DOI: 10.1021/acscombsci.5b00155
ACS Comb. Sci. 2016, 18, 444−455

because of the very small size of crystals available. Corrections were made for synchrotron beam decay and for absorption and other systematic effects on the basis of repeated and equivalent data. The structures were solved by direct methods and refined on all unique F^2 values with anisotropic non-hydrogen atoms, with freely refined isotropic H atoms bonded to N, and with a riding model for H atoms bonded to C. All four structures are fully ordered; **3i** have two independent molecules in the asymmetric unit, and the noncentrosymmetric but achiral crystal structure of **3i** displays inversion twinning with essentially equal components. Full crystallographic details are given in the Supporting Information. Programs were standard Oxford Diffraction CrysAlisPro[38] and Bruker Apex2[39] for data collection and processing, and SHELXTL[40] and SHELXL-2014_ENREF_52_ENREF_53[41] for structure solution and refinement. CCDC references: 1410001, 141003, and 1410004.

■ ASSOCIATED CONTENT

Supporting Information

The Supporting Information is available free of charge on the ACS Publications website at DOI: 10.1021/acscombsci.5b00155.

Additional screening and synthesis information, X-ray crystal structure data for compounds **12a**, **3a**, and **3i**, synthetic procedures, ERK5 and p38α LANCE assay protocols, kinase selectivity data for **6h**. (PDF)

Crystallographic information file for compounds **12a**, **3a**, and **3i** (CIF)

■ AUTHOR INFORMATION

Corresponding Author

*E-mail: Ian.Hardcastle@ncl.ac.uk.

Funding

This work was supported by Cancer Research UK (C240/A7409, C1296/A6963 and C2115/A21421), EPSRC equipment grant (EP/F03637X/1), and the synchrotron component of the UK National Crystallography Service 2001−2010 (EP/D07746X/1).

Notes

The authors declare no competing financial interest.

■ ACKNOWLEDGMENTS

We thank CCLRC for access to synchrotron diffraction facilities at SRS. The use of the EPSRC National Mass Spectroscopy Facility, Swansea University is gratefully acknowledged.

■ REFERENCES

(1) (a) Zhou, G.; Bao, Z. Q.; Dixon, J. E. Components of a New Human Protein Kinase Signal Transduction Pathway. *J. Biol. Chem.* **1995**, *270* (21), 12665−12669. (b) Zhou, G. C.; Bao, A.; Guan, K. L.; Dixon, J. E. Specifical Interactions Between Newly Identified Human Kinases, Mek5 And Erk5. *FASEB J.* **1995**, *9* (6), A1306−A1306. (c) Abe, J.; Kusuhara, M.; Ulevitch, R. J.; Berk, B. C.; Lee, J. D. Big mitogen-activated protein kinase 1 (BMK1) is a redox-sensitive kinase. *J. Biol. Chem.* **1996**, *271* (28), 16586−16590.

(2) Hayashi, M.; Lee, J. D. Role of the BMK1/ERK5 signaling pathway: lessons from knockout mice. *J. Mol. Med.* **2004**, *82* (12), 800−8.

(3) English, J. M.; Pearson, G.; Hockenberry, T.; Shivakumar, L.; White, M. A.; Cobb, M. H. Contribution of the ERK5/MEK5 pathway to Ras/Raf signaling and growth control. *J. Biol. Chem.* **1999**, *274* (44), 31588−92.

(4) Wang, X.; Tournier, C. Regulation of cellular functions by the ERK5 signalling pathway. *Cell. Signalling* **2006**, *18* (6), 753−60.

(5) Roberts, O. L.; Holmes, K.; Muller, J.; Cross, D. A.; Cross, M. J. ERK5 and the regulation of endothelial cell function. *Biochem. Soc. Trans.* **2009**, *37* (Pt 6), 1254−9.

(6) (a) Kato, Y.; Kravchenko, V. V.; Tapping, R. I.; Han, J.; Ulevitch, R. J.; Lee, J.-D. BMK1/ERK5 regulates serum-induced early gene expression through transcription factor MEF2C. *EMBO J.* **1997**, *16* (23), 7054−7066. (b) Yang, C. C.; Ornatsky, O. I.; McDermott, J. C.; Cruz, T. F.; Prody, C. A. Interaction of myocyte enhancer factor 2 (MEF2) with a mitogen-activated protein kinase, ERK5/BMK1. *Nucleic Acids Res.* **1998**, *26* (20), 4771−4777. (c) Kato, Y.; Tapping, R. I.; Huang, S.; Watson, M. H.; Ulevitch, R. J.; Lee, J.-D. Bmk1/Erk5 is required for cell proliferation induced by epidermal growth factor. *Nature* **1998**, *395* (6703), 713−716. (d) English, J. M.; Pearson, G.; Baer, R.; Cobb, M. H. Identification of Substrates and Regulators of the Mitogen-activated Protein Kinase ERK5 Using Chimeric Protein Kinases. *J. Biol. Chem.* **1998**, *273* (7), 3854−3860. (e) Kamakura, S.; Moriguchi, T.; Nishida, E. Activation of the Protein Kinase ERK5/BMK1 by Receptor Tyrosine Kinases. *J. Biol. Chem.* **1999**, *274* (37), 26563−26571. (f) Pearson, G.; English, J. M.; White, M. A.; Cobb, M. H. ERK5 and ERK2 Cooperate to Regulate NF-κB and Cell Transformation. *J. Biol. Chem.* **2001**, *276* (11), 7927−7931. (g) Terasawa, K.; Okazaki, K.; Nishida, E. Regulation of c-Fos and Fra-1 by the MEK5-ERK5 pathway. *Genes Cells* **2003**, *8* (3), 263−273.

(7) (a) Hayashi, M.; Fearns, C.; Eliceiri, B.; Yang, Y.; Lee, J. D. Big mitogen-activated protein kinase 1/extracellular signal-regulated kinase 5 signaling pathway is essential for tumor-associated angiogenesis. *Cancer Res.* **2005**, *65* (17), 7699−7706. (b) Le, N.-T; Heo, K.-S.; Takei, Y.; Lee, H.; Woo, C.-H.; Chang, E.; McClain, C.; Hurley, C.; Wang, X.; Li, F.; Xu, H.; Morrell, C.; Sullivan, M. A.; Cohen, M. S.; Serafimova, I. M.; Taunton, J.; Fujiwara, K.; Abe, J.-I. A Crucial Role for p90RSK-Mediated Reduction of ERK5 Transcriptional Activity in Endothelial Dysfunction and Atherosclerosis. *Circulation* **2013**, *127* (4), 486. (c) Ranganathan, A.; Pearson, G. W.; Chrestensen, C. A.; Sturgill, T. W.; Cobb, M. H. The MAP kinase ERK5 binds to and phosphorylates p90 RSK. *Arch. Biochem. Biophys.* **2006**, *449* (1−2), 8−16.

(8) (a) Drew, B. A.; Burow, M. E.; Beckman, B. S. MEK5/ERK5 pathway: the first fifteen years. *Biochim. Biophys. Acta, Rev. Cancer* **2012**, *1825* (1), 37−48. (b) Lochhead, P. A.; Gilley, R.; Cook, S. J. ERK5 and its role in tumour development. *Biochem. Soc. Trans.* **2012**, *40* (1), 251−6.

(9) (a) Mehta, P. B.; Jenkins, B. L.; McCarthy, L.; Thilak, L.; Robson, C. N.; Neal, D. E.; Leung, H. Y. MEK5 overexpression is associated with metastatic prostate cancer, and stimulates proliferation, MMP-9 expression and invasion. *Oncogene* **2003**, *22* (9), 1381−1389. (b) McCracken, S. R.; Ramsay, A.; Heer, R.; Mathers, M. E.; Jenkins, B. L.; Edwards, J.; Robson, C. N.; Marquez, R.; Cohen, P.; Leung, H. Y. Aberrant expression of extracellular signal-regulated kinase 5 in human prostate cancer. *Oncogene* **2008**, *27* (21), 2978−88.

(10) Montero, J. C.; Ocana, A.; Abad, M.; Ortiz-Ruiz, M. J; Pandiella, A.; Esparis-Ogando, A. Expression of ERK5 in Early Stage Breast Cancer and Association with Disease Free Survival Identifies this Kinase as a Potential Therapeutic Target. *PLoS One* **2009**, *4* (5), e5565.

(11) Zen, K.; Yasui, K.; Nakajima, T.; Zen, Y.; Zen, K.; Gen, Y.; Mitsuyoshi, H.; Minami, M.; Mitsufuji, S.; Tanaka, S.; Itoh, Y.; Nakanuma, Y.; Taniwaki, M.; Arii, S.; Okanoue, T.; Yoshikawa, T. ERK5 is a target for gene amplification at 17p11 and promotes cell growth in hepatocellular carcinoma by regulating mitotic entry. *Genes, Chromosomes Cancer* **2009**, *48* (2), 109−120.

(12) Arias-González, L.; Moreno-Gimeno, I.; del Campo, A. R.; Serrano-Oviedo, L.; Valero, M. L.; Esparís-Ogando, A.; de la Cruz-Morcillo, M. Á.; Melgar-Rojas, P.; García-Cano, J.; Cimas, F. J.; Hidalgo, M. J. R.; Prado, A.; Callejas-Valera, J. L.; Nam-Cha, S. H.; Giménez-Bachs, J. M.; Salinas-Sánchez, A. S.; Pandiella, A.; del Peso, L.; Sánchez-Prieto, R. ERK5/BMK1 Is a Novel Target of the Tumor Suppressor VHL: Implication in Clear Cell Renal Carcinoma. *Neoplasia* **2013**, *15* (6), 649−659.

(13) Tatake, R. J.; O'Neill, M. M.; Kennedy, C. A.; Wayne, A. L.; Jakes, S.; Wu, D.; Kugler, S. Z., Jr; Kashem, M. A.; Kaplita, P.; Snow, R. J.

Identification of pharmacological inhibitors of the MEK5/ERK5 pathway. *Biochem. Biophys. Res. Commun.* **2008**, *377* (1), 120−125.
(14) Yang, Q.; Deng, X.; Lu, B.; Cameron, M.; Fearns, C.; Patricelli, M. P.; Yates, J. R.; Gray, N. S.; Lee, J.-D. Pharmacological Inhibition of BMK1 Suppresses Tumor Growth through Promyelocytic Leukemia Protein. *Cancer Cell* **2010**, *18* (4), 396.
(15) Elkins, J. M.; Wang, J.; Deng, X.; Pattison, M. J.; Arthur, J. S. C.; Erazo, T.; Gomez, N.; Lizcano, J. M.; Gray, N. S.; Knapp, S. X-ray Crystal Structure of ERK5 (MAPK7) in Complex with a Specific Inhibitor. *J. Med. Chem.* **2013**, *56* (11), 4413−4421.
(16) Sureban, S. M.; May, R.; Weygant, N.; Qu, D.; Chandrakesan, P.; Bannerman-Menson, E.; Ali, N.; Pantazis, P.; Westphalen, C. B.; Wang, T. C.; Houchen, C. W. XMD8−92 inhibits pancreatic tumor xenograft growth via a DCLK1-dependent mechanism. *Cancer Lett.* **2014**, *351* (1), 151−161.
(17) Rovida, E.; Di Maira, G.; Tusa, I.; Cannito, S.; Paternostro, C.; Navari, N.; Vivoli, E.; Deng, X.; Gray, N. S.; Esparís-Ogando, A.; David, E.; Pandiella, A.; Dello Sbarba, P.; Parola, M.; Marra, F. The mitogen-activated protein kinase ERK5 regulates the development and growth of hepatocellular carcinoma. *Gut* **2015**, *64* (9), 1454−1465.
(18) Finegan, K. G.; Perez-Madrigal, D.; Hitchin, J. R.; Davies, C. C.; Jordan, A. M.; Tournier, C. ERK5 Is a Critical Mediator of Inflammation-Driven Cancer. *Cancer Res.* **2015**, *75* (4), 742−753.
(19) (a) Collins, I.; Workman, P. New approaches to molecular cancer therapeutics. *Nat. Chem. Biol.* **2006**, *2* (12), 689−700. (b) Hughes, J. P.; Rees, S.; Kalindjian, S. B.; Philpott, K. L. Principles of early drug discovery. *Br. J. Pharmacol.* **2011**, *162* (6), 1239−1249.
(20) (a) Barton, D.; Ollis, W. D. *Heterocyclic Compounds*; Pergamon: Oxford, NY, 1979; Vol. *4*. (b) Jordan, A. D.; Luo, C.; Reitz, A. B. Efficient Conversion of Substituted Aryl Thioureas to 2-Aminobenzothiazoles Using Benzyltrimethylammonium Tribromide. *J. Org. Chem.* **2003**, *68* (22), 8693−8696. (c) Ding, Q.; He, X.; Wu, J. Synthesis of 2-Aminobenzothiazole via Copper(I)-Catalyzed Tandem Reaction of 2-Iodobenzenamine with Isothiocyanate. *J. Comb. Chem.* **2009**, *11* (4), 587−591. (d) Li, Z.; Xiao, S.; Tian, G.; Zhu, A.; Feng, X.; Liu, J. Microwave Promoted Environmentally Benign Synthesis of 2-Amino-benzothiazoles and Their Urea Derivatives. *Phosphorus, Sulfur Silicon Relat. Elem.* **2008**, *183* (5), 1124−1133. (e) Jordan, A. D.; Luo, C.; Reitz, A. B. Efficient Conversion of Substituted Aryl Thioureas to 2-Aminobenzothiazoles Using Benzyltrimethylammonium Tribromide. *J. Org. Chem.* **2003**, *68* (22), 8693−8696.
(21) Nagarajan, S. R.; De Crescenzo, G. A.; Getman, D. P.; Lu, H.-F.; Sikorski, J. A.; Walker, J. L.; McDonald, J. J.; Houseman, K. A.; Kocan, G. P.; Kishore, N.; Mehta, P. P.; Funkes-Shippy, C. L.; Blystone, L. Discovery of novel benzothiazolesulfonamides as potent inhibitors of HIV-1 protease. *Bioorg. Med. Chem.* **2003**, *11* (22), 4769−4777.
(22) Shestopalov, A. M.; Nikishin, K. G. One stage synthesis of 4,6-diaryl-3-cyanopyridine-2(1H)-thiones. *Chem. Heterocycl. Compd.* **1998**, *34*, 1093.
(23) Hepworth, J. D. Aminoacetone Semicarbazone Hydrochloride. *Organic Syntheses, Coll. Vol.* **1973**, *5*, 27.
(24) Schmidt, H.-W.; Koitz, G.; Junek, H. A convenient synthesis of 2-substituted 4-amino-5-pyrimidinecarbonitriles. *J. Heterocycl. Chem.* **1987**, *24* (5), 1305−1307.
(25) Ranu, B. C.; Dutta, J.; Guchhait, S. K. Indium metal as a reducing agent. Selective reduction of the carbon−carbon double bond in highly activated conjugated alkenes. *Org. Lett.* **2001**, *3* (16), 2603−2605.
(26) Corey, E. J.; Chaykovsky, M. Dimethyloxosulfonium methylide ($(CH_3)_2SOCH_2$) and dimethylsulfonium methylide ($(CH_3)_2SCH_2$). Formation and application to organic synthesis. *J. Am. Chem. Soc.* **1965**, *87* (6), 1353−1364.
(27) Ciaccio, J. A.; Aman, C. E. Instant Methylide" Modification of the Corey−Chaykovsky Cyclopropanation Reaction. *Synth. Commun.* **2006**, *36* (10), 1333−1341.
(28) Wu, Q.; Caine, J. M.; Thomson, S. A.; Slavica, M.; Grunewald, G. L.; McLeish, M. J. Time-dependent inactivation of human phenylethanolamine N-methyltransferase by 7-isothiocyanatotetrahydroisoquinoline. *Bioorg. Med. Chem. Lett.* **2009**, *19* (4), 1071−1074.
(29) Devine, S. M.; Mulcair, M. D.; Debono, C. O.; Leung, E. W. W.; Nissink, J. W. M.; Lim, S. S.; Chandrashekaran, I. R.; Vazirani, M.; Mohanty, B.; Simpson, J. S.; Baell, J. B.; Scammells, P. J.; Norton, R. S.; Scanlon, M. J. Promiscuous 2-Aminothiazoles (PrATs): A Frequent Hitting Scaffold. *J. Med. Chem.* **2015**, *58* (3), 1205−1214.
(30) Baell, J. B.; Holloway, G. A. New Substructure Filters for Removal of Pan Assay Interference Compounds (PAINS) from Screening Libraries and for Their Exclusion in Bioassays. *J. Med. Chem.* **2010**, *53* (7), 2719−2740.
(31) Trist, I. M. L.; Nannetti, G.; Tintori, C.; Fallacara, A. L.; Deodato, D.; Mercorelli, B.; Palù, G.; Wijtmans, M.; Gospodova, T.; Edink, E.; Verheij, M.; de Esch, I.; Viteva, L.; Loregian, A.; Botta, M. 4,6-Diphenylpyridines as Promising Novel Anti-Influenza Agents Targeting the PA−PB1 Protein−Protein Interaction: Structure−Activity Relationships Exploration with the Aid of Molecular Modeling. *J. Med. Chem.* **2016**, *59* (6), 2688−2703.
(32) Thomas, A. P. Preparation and formulation of 4-amino-5-cyano-2-anilino-pyrimidines as inhibitors of cell-cycle kinases for pharmaceutical use in the treatment of cancer Int. Patent WO 1998033798 A2, 2001
(33) Marchetti, F.; Cano, C.; Curtin, N. J.; Golding, B. T.; Griffin, R. J.; Haggerty, K.; Newell, D. R.; Parsons, R. J.; Payne, S. L.; Wang, L. Z.; Hardcastle, I. R. Synthesis and biological evaluation of 5-substituted O4-alkylpyrimidines as CDK2 inhibitors. *Org. Biomol. Chem.* **2010**, *8* (10), 2397−2407.
(34) Down, K.; Bamborough, P.; Alder, C.; Campbell, A.; Christopher, J. A.; Gerelle, M.; Ludbrook, S.; Mallett, D.; Mellor, G.; Miller, D. D.; Pearson, R.; Ray, K.; Solanke, Y.; Somers, D. The discovery and initial optimization of pyrrole-2-carboxamides as inhibitors of p38[alpha] MAP kinase. *Bioorg. Med. Chem. Lett.* **2010**, *20* (13), 3936−3940.
(35) Workman, P.; Collins, I. Probing the Probes: Fitness Factors For Small Molecule Tools. *Chem. Biol.* **2010**, *17* (6), 561−577.
(36) Reuillon, T.; Miller, D.; Myers, S.; Molyneux, L.; Cano, C.; Hardcastle, I. R.; Griffin, R. J.; Rigoreau, L.; Golding, B. T.; Noble, M. E. N. Pyrrolcarboxamide Derivatives For The Inhibition of ERK5. Int Patent WO/2016/042341.
(37) *Prism*, version 6; GraphPad Software Inc., 2014.
(38) *CrysAlisPro*; Oxford Diffraction: Oxford, UK, 2008.
(39) *Apex2*; Bruker AXS Inc.: Madison, MI, USA, 2008.
(40) Sheldrick, G. A short history of SHELX. *Acta Crystallogr., Sect. A: Found. Crystallogr.* **2008**, *64* (1), 112−122.
(41) Sheldrick, G. Crystal structure refinement with SHELXL. *Acta Crystallogr., Sect. C: Struct. Chem.* **2015**, *71* (1), 3−8.

DOI: 10.1021/acscombsci.5b00155
ACS Comb. Sci. 2016, 18, 444−455